The Positive Effect of Formaldehyde on the Photocatalytic Renoxification of Nitrate on TiO_2 Particles

Yuhan Liu, Xuejiao Wang, Mengshuang Sheng, Chunxiang Ye, Jing Shang*

State Key Joint Laboratory of Environmental Simulation and Pollution Control, College of Environmental Sciences and Engineering, Peking University, 5 Yiheyuan Road, Beijing 100871, P. R. China

Corresponding author: Jing Shang

Email: shangjing@pku.edu.cn

Abstract

Renoxification is the process of recycling of NO_3^-/HNO_3 into NO_x under illumination, which is mostly ascribed to the photolysis of nitrate. TiO_2, a typical mineral dust component, can play its photocatalytic role in "renoxification" process due to NO_3 radical formed, and we define this process as "photocatalytic renoxification". Formaldehyde (HCHO), the most abundant carbonyl compound in the atmosphere, may participate in the renoxification of nitrate-doped TiO_2 particles. In this study, we established an environmental chamber reaction system with the presence of HCHO and nitrate-doped TiO_2. The direct photolyses of both nitrate and NO_3 radical were excluded by adjusting the illumination wavelength, so as to explore the effect of HCHO on the "photocatalytic renoxification". It is found that NO_x

Formatted: Indent: First line: 2 ch

concentration can reach up to more than 100 ppb for nitrate-doped TiO_2 particles, while almost no NO_x was generated in the absence of HCHO. Nitrate type, relative humidity and HCHO concentration were found to influence NO_x release. Adsorbed HCHO may react with nitrate radicals through hydrogen abstraction to form adsorbed HNO_3 on the surface, which is responsible for the release of NO_x. The mass generation of NO_x was suggested to via the NO_3^--NO_3·-HCHO-HNO_3-NO_x pathway, with HCHO and TiO_2 exhibiting a significant synergistic effect. Our proposed reaction mechanism by which HCHO promotes photocatalytic renoxification is helpful for deeply understanding the atmospheric photochemical processes and nitrogen cycling.~~Renoxification is the recycling of NO_3^-/HNO_3 into NO_x under illumination; it is promoted by the photocatalysis of TiO_2. Formaldehyde (HCHO), the most abundant carbonyl compound in the atmosphere, may participate in the renoxification of nitrate-doped TiO_2 (NO_3^--TiO_2) aerosols. In this study, we established an environmental chamber reaction system under different light sources, excluding direct photolysis of nitrate by adjusting the illumination wavelength, to explore the photocatalytic renoxification process. It is suggested that HCHO and TiO_2 have a significant synergistic effect on photocatalytic renoxification via the NO_3^--NO_3·-HCHO-HNO_3-NO_x pathway. Adsorbed HCHO may react with nitrate radicals through hydrogen abstraction to form HNO_3 on the surface, resulting in the mass generation of NO_x. We found that for 4 wt% NO_3^--TiO_2 aerosols (e.g., KNO_3-TiO_2), the NO_x concentration reached up to 110 ppb, and was 2 orders of magnitude higher than in the absence of HCHO. Nitrate type and contents, relative~~

~~humidity, and HCHO concentration were found to influence NO_x release. The significant synergistic enhancement effect of renoxification affects photochemical processes such as atmospheric oxidation and nitrogen cycling on the surfaces of particles containing semiconductor oxides, with the participation of hydrogen donor organics.~~

Formatted: Indent: First line: 2 ch

1 Introduction

The levels of ozone (O_3) and hydroxyl radicals (·OH) in the troposphere can be promoted by nitrogen oxides (NO_x = NO + NO_2), such that NO_x plays an important role in the formation of secondary aerosols and atmospheric oxidants (Platt et al., 1980; Stemmler et al., 2006; Harris et al., 1982; Finlayson-Pitts and Pitts, 1999). NO_x can be converted into nitric acid (HNO_3) and nitrate (NO_3^-) through a series of oxidation and hydrolysis reactions and is eventually removed from the atmosphere through subsequent wet or dry deposition (Dentener and Crutzen, 1993; Goodman et al., 2001; Monge et al., 2010; Bedjanian and El Zein, 2012). However, comparisons of observations and modeling results for the marine boundary layer, land, and free troposphere (Read et al., 2008; Lee et al., 2009; Seltzer et al., 2015) have shown underestimation of HNO_3 or NO_3^- content, NO_x abundance, and NO_x/HNO_3 ratios, indicating the presence of a new, rapid NO_x circulation pathway (Ye et al., 2016b; Reed et al., 2017). Some researchers have suggested that deposited NO_3^- and HNO_3 can be recycled back to gas phase NO_x under illumination, via the renoxification process (Schuttlefield et al., 2008; Romer et al., 2018; Bao et al., 2020; Shi et al.,

2021). Photolytic renoxification occurs under light with a wavelength of < 350 nm, through the photolysis of NO_3^-/HNO_3 adsorbed on the solid surface to generate NO_x. Notably, the photolysis of $NO_3^-HNO_3$ is reported to occur at least 2 orders of magnitude faster on different solid surfaces (natural or artificial) or aerosols than in the gas phase (Ye et al., 2016a; Zhou et al., 2003; Baergen and Donaldson, 2013). Several recent studies have shown that renoxification has important atmospheric significance (Deng et al., 2010; Kasibhatla et al., 2018; Romer et al., 2018; Alexander et al., 2020), providing the atmosphere with a new source of photochemically reactive nitrogen species, i.e., HONO or NO_x, resulting in the production of more photooxidants such as O_3 or ·OH (Ye et al., 2017), which further oxidize volatile organic compounds (VOCs), leading to the formation of more chromophores, thereby affecting the photochemical process (Bao et al., 2020).

Renoxification processes have recently been observed on different types of atmospheric particles, such as urban grime and mineral dust (Ninneman et al., 2020; Bao et al., 2018; Baergen and Donaldson, 2013; Ndour et al., 2009). Atmospheric titanium dioxide (TiO_2) is mainly derived from windblown mineral dust, with mass mixing ratios ranging from 0.1 to 10% (Chen et al., 2012). TiO_2 is widely used in industrial processes and building exteriors for its favorable physical and chemical properties. Titanium and nitrate ions have been found to coexist in atmospheric particulates in different regions worldwide (Sun et al., 2005; Schwartz-Narbonne et al., 2019). The relative content of TiO_2 and NO_3^- in atmospheric particles varies greatly, and nitrate-coated TiO_2 (NO_3^--TiO_2) aerosols containing TiO_2 as the main body can

be used to effectively represent particles for sandstorm modeling (Sun et al., 2005; Kim et al., 2012). TiO_2 is a semiconductor metal oxide that can facilitate the photolysis of nitrate and the release of NO_x due to its photocatalytic activity (Ndour et al., 2009; Chen et al., 2012; Verbruggen, 2015; Schwartz-Narbonne et al., 2019). Under ultraviolet (UV) light, TiO_2 generates electron-hole pairs in the conduction and valence bands, respectively (Linsebigler et al., 1995). Nitrate ions adsorbed at the oxide surface react with the photogenerated holes (h^+) to form nitrate radicals ($NO_3\cdot$), which are subsequently photolyzed to NO_x, mainly under visible light illumination (Schuttlefield et al., 2008; George et al., 2015; Schwartz-Narbonne et al., 2019). Thus, the renoxification of NO_3^- is faster on TiO_2 than on other oxides in mineral dust aerosols such as SiO_2 or Al_2O_3 (Lesko et al., 2015; Ma et al., 2021). In this study, we refer to renoxification involving h^+ and NO_3^- in the reaction as photocatalytic renoxification based on the photocatalytic properties of TiO_2.

Many previous studies have focused mainly on particulate nitrate-NO_x photochemical cycling reactions, despite the potential impact of other reactant gases in the atmosphere. Formaldehyde (HCHO), the most abundant carbonyl compound in the atmosphere, which can react at night with $NO_3\cdot$ via hydrogen abstraction reactions to form HNO_3 (Atkinson, 1991). Our previous study showed that the degradation rate of HCHO was faster on NO_3^--TiO_2 aerosols than on TiO_2 particles, perhaps as a result of HCHO oxidation by $NO_3\cdot$(Shang et al., 2017). To date, no studies have reported the effect of HCHO on photocatalytic renoxification. Adsorbed HCHO would react with $NO_3\cdot$ generated on the NO_3^--TiO_2 aerosol surface, thus alter the surface nitrogenous

species and renoxification process. The present study is the first to explore the combined effect of HCHO and photocatalytic TiO_2 particles on the renoxification of nitrate. The wavelengths of the light sources were adjusted to exclude photolytic renoxification while making photocatalytic renoxification available for better elucidate the reaction mechanism. We investigated the effects of various influential factors including nitrate type, nitrate content, RH, and initial HCHO concentration, to understand the atmospheric renoxification of nitrate in greater detail.

2 Methods

2.1 Environmental chamber setup

Details of the experimental apparatus and protocol used in the current study have been previously described (Shang et al., 2017). Briefly, the main body of the environmental chamber is a 400 L polyvinyl fluoride (PVF) bag filled with synthetic air (high purity N_2 (99.999%) mixed with high purity O_2 (99.999%) in the ratio of 79:21 by volume, Beijing Huatong Jingke Gas Chemical Co.). The chamber is capable of temperature (~293 K) and relative humidity (0.8–70%) control using a water bubbler and air conditioners, respectively. The chamber is equipped with two light sources both with the central wavelength of 365 nm. One is a set of 36 W tube lamps with a main spectrum of 320–400 nm and a small amount of 480-600 nm visible light (Figure S1a). The other is a set of 12 W Light-emitting diode (LED) lamps with a narrow main spectrum of 350-390 nm (Figure S1b). The light intensities for the tube and LED lamp at 365 nm were 300 $\mu W \cdot cm^{-2}$ and 200 $\mu W \cdot cm^{-2}$, respectively, measured in the middle of the chamber. NO_x concentrations at the outlet

of the chamber were monitored by a chemiluminescence NO_x analyzer (ECOTECH, EC9841B). HCHO was generated by thermolysis of paraformaldehyde at 70 °C and detected via acetyl acetone spectrophotometric method using a UV-Vis spectrophotometer (PERSEE, T6) or a fluorescence spectrophotometer (THERMO, Lumina), depending on different initial HCHO concentrations. The particle size distribution was measured by a Scanning Nano Particle Spectrometer (HCT, SNPS-20). Electron Spin Resonance (Nuohai Life Science, MiniScope MS 5000) was used to measure ·OH on the surface of particles. 5,5-dimethl-1-pyrroline-N-oxide (DPMO, Enzo) was used as the capture agent. 50 μL particle-containing suspension mixed with 50 μL DMPO (concentration of 200 μM) was loaded in a 1 mm capillary. Four 365 nm LED lamps were placed side by side vertically at a distance of about 1 cm from the capillary, and the measurement was carried out after 1 min of irradiation. The modulation frequency was 100 kHz, the modulation amplitude was 0.2 mT, the microwave power was 10 mW and the sweep time was 60 s.

2.2 Nitrate-TiO_2 composite samples

In our experiments, two nitrate salts, potassium nitrate (AR, Beijing Chemical Works Co., Ltd) or ammonium nitrate (AR, Beijing Chemical Works Co., Ltd), were complexed with pure TiO_2 (≥ 99.5%, Degussa AG) powder or TiO_2 (1 wt.%)/SiO_2 mixed powder to prepare NO_3^--TiO_2 or NO_3^--TiO_2 (1 wt.%)/SiO_2 samples. 250 mg TiO_2 was simply mixed in nitrate solutions at the desired mass mixing ratio (with nitrate content of ~~1 wt.%,~~ 4 wt.%~~, 20 wt.%, 80 wt.% and 95 wt.%~~) to obtain a mash. The mash was dried at 90 °C and then ground carefully for 30 min. A series of

samples with different amount of nitrate were prepared and diffuse reflectance fourier transform infrared spectroscopy (DRIFTS) measurements were made to test their homogeneity. Figure S2 shows DRIFTS spectra of these KNO_3-TiO_2 composites, of which 1760 cm^{-1} peak is one of the typical vibrating peaks of nitrate (Aghazadeh, 2016; Maeda et al., 2011). Ratio value of peak area from 1730-1790 cm^{-1} for 1, 4, 32, 80 wt.% composited samples is 1: 4.1: 29.8: 81.6, which is very close to that of theoretical value, proving that the samples were uniformly mixed. ~~The mash was dried at 90 °C and then ground carefully to ensure a uniform composite of particles.~~ SiO_2 (AR, Xilong Scientific Co., Ltd.) with no optical activity was also chosen for comparison, and samples of KNO_3-SiO_2 and KNO_3-TiO_2(1 wt.%)/SiO_2 samples with a potassium nitrate content of 4 wt.% were prepared. The blank 250 mg TiO_2 sample was solved in pure water with the same procedure as mentioned above. 4 wt.% HNO_3-TiO_2 composite particles were prepared for comparison. Concentrated nitric acid (AR, Beijing Chemical Works Co., Ltd) was diluted to 1 M and 250 mg TiO_2 was added to the nitric acid solution and stirred evenly. A layer of aluminum foil was covered on the surface of the HNO_3-TiO_2 homogenate and dried naturally in the room. After air-drying, follow the same steps above to grind for use. We also selected Arizona Test Dust (ATD, Powder Technology Inc.), whose chemical composition and weight percentage were shown in Table S1, as a substitute of NO_3^-/TiO_2 to investigate the "photocatalytic renoxification" process of nitrate and the positive effect of HCHO.

2.3 Environmental chamber experiments

For the chamber operation, we completely evacuated the chamber after every

experiment, then cleaned the chamber walls with deionized water and then dried by flushing the chamber with ultra-zero air to remove any particles or gases collected on the chamber walls. The experiments carried out in the environmental chamber can be divided into two categories according to whether HCHO was involved or not. (1) No HCHO involvement in the reaction. The PVF bag was inflated by 260 L synthetic air, and then 75 mg particles were instantly sprayed into the chamber by a transient high-pressure airflow. ~~then 75 mg TiO_2 particles were sprayed into PVF bag.~~ As shown in Figure S~~2~~3, the concentration of ~~the~~ 4 wt.% KNO_3-TiO_2 particles decreased rapidly due to the sedimentation of the larger particles and the electrostatic adsorption of the particles by the environmental chamber. The size distribution ~~of TiO_2~~ reached stable after about 60 min with the peak particle size was about 120 nm, similar to that of atmospheric particles in some urban areas in China (Wang et al., 2015; Li et al., 2019). ~~The size distribution could maintain for more than 4 hours, with the number concentration in the chamber decreased by no more than 5% per hour.~~ (2) With the participation of HCHO. The PVF bag was inflated by 125 L synthetic air, followed by the introduction of HCHO, and then the chamber was filled up with zero air to about 250 L. In order to know the HCHO adsorption before and after the particles' introduction, we conducted a conditional experiment in the dark. It can be seen from Figure S4 that it took about 90 min for the concentration of HCHO to reach stable, and can be sustained. ~~It can be seen from Figure S3 that it took about 60 min for the HCHO concentration to reach stable.~~ Then, 75 mg TiO_2 or NO_3^-/TiO_2 powders were introduced instantly and the concentration of HCHO decreased upon the introduction.

It took about ~~another~~ 60 min for HCHO to reach its second adsorption equilibrium, and the concentration of HCHO can be stable for several hours in the dark. Therefore, for the irradiation experiments, the particles were injected at 90 min after HCHO's introduction, and the lamps were turned on at 60 min after the particle's introduction.~~for HCHO concentration to get stable. After the concentrations of both HCHO and aerosol became stable, the lamps were turned on and the concentrations of NO_x were monitored.~~

To determine the background value of NO_x in the reaction system, four blank experiments were carried out under illumination without nitrate: "synthetic air", "synthetic air + TiO_2", "synthetic air + HCHO" and "synthetic air + HCHO + TiO_2". In the blank experiments of "synthetic air" and "synthetic air + TiO_2", the NO_x concentration remained stable during 180 min illumination, and the concentration change was no more than 0.5 ppb (Figure S45a). Therefore, the environmental chamber, synthetic air and the surface of TiO_2 particles were thought to be relatively clean, and there was no generation and accumulation of NO_x under illumination. When HCHO was introduced into the environmental chamber, NO_x accumulated ~2 ppb in 120 min with or without TiO_2 particles (Figure S45b). Compared with the blank experiment results when there was no HCHO, NO_x might come from the generation process of HCHO (impurities in paraformaldehyde). However, considering the high concentration level of NO_x produced in the NO_3^--TiO_2 system containing HCHO under the same conditions in this study (see later in Figure 2), the NO_x generated in this blank experiment can be negligible.

3 Results and discussion

3.1 The positive effect of TiO_2 on the renoxification process

We investigated the photocatalytic role of TiO_2 on renoxification. The light source was two 365 nm tube lamps containing small amounts of 400–600 nm visible light; this setup was suitable for exciting TiO_2 and the photolysis of available nitrate radicals. Raw NO_x data measured in the chamber under dark and illuminated conditions for 4 wt.% KNO_3-SiO_2 and 4 wt.% KNO_3-TiO_2 (1 wt.%)/SiO_2 are shown in Figure 1. The ratio of 1 wt. % TiO_2 to SiO_2 corresponds to their ratio in sand and dust particles. We observed no NO_x in the KNO_3-SiO_2 sample under dark or illumination, indicating very weak direct photolysis of nitrate under our 365 nm tube-lamp illumination conditions. However, when the sample containing TiO_2/SiO_2 was illuminated, NO_x continually accumulated in the chamber. This finding confirms that NO_x production arising from photodissociation of NO_3^- on TiO_2/SiO_2 was caused by the photocatalytic property of TiO_2 (i.e., photocatalytic renoxification) and was not due to the direct photolysis of NO_3^- (photolytic renoxification).

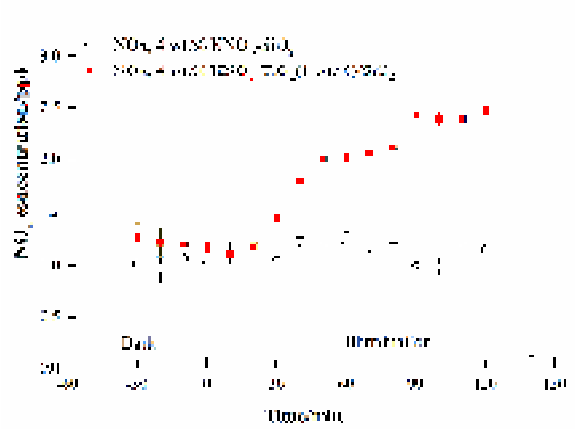

Figure 1. Effect of illumination on the release of NO_x from 4 wt.% KNO_3-SiO_2 and 4 wt.% KNO_3-TiO_2(1 wt.%)/SiO_2 at 293 K and 0.8% of relative humidity. 365 nm tube lamps were used during the illumination experiments.

TiO_2 can be excited by UV illumination to generate electron-hole pairs, and the h^+ can react with adsorbed NO_3^- to produce $NO_3\cdot$ (Ndour et al., 2009). Thus, in the present study, $NO_3\cdot$ mainly absorbed visible light emitted from the tube lamps, which was subsequently photolyzed to NO_x through Eqs. (3) and (4) (Wayne et al., 1991), which explains why NO_x was observed in this study. Thus, we demonstrated that TiO_2 can be excited at illumination wavelengths of ~365 nm, even when then content was very low, and that NO_x accumulated due to the production and further phytolysis of $NO_3\cdot$. However, the production rate of NO_x was very slow, reaching only 1.3 ppb during 90 min of illumination. This result may have been caused by the blocking effect of K^+ on NO_3^-. K^+ forms ion pairs with NO_3^-, and electrostatic repulsion between K^+ and h^+ prevents NO_3^- from combining with h^+ to generate $NO_3\cdot$ to a certain extent, thereby weakening the positive effect of TiO_2 on the renoxification of KNO_3 (Rosseler et al., 2013).

$$TiO_2 + h\upsilon\ (\lambda < 390\ nm) \rightarrow e^- + h^+ \quad (1)$$

$$NO_3^- + h^+ \rightarrow NO_3\cdot \quad (2)$$

$$NO_3\cdot + h\upsilon\ (\lambda < 640\ nm) \rightarrow NO_2 + O\cdot \quad (3)$$

$$NO_3\cdot + h\upsilon\ (585\ nm < \lambda < 640\ nm) \rightarrow NO + O_2 \quad (4)$$

3.2 The synergistic positive effect of TiO_2 and HCHO on the renoxification process

LED lamps with a wavelength range of 350–390 nm and no visible light were used to irradiate 4 wt.% KNO_3-TiO_2 without generating NO_x (NO_2 and NO concentrations fluctuate within the error range of the instrument) (Figure S~~5~~6). TiO_2 can be excited under this range of irradiation, producing NO_3 radicals as discussed above. The lack of NO_x generation indicates that neither nitrate photolysis nor NO_3· photolysis occurred under 365 nm LED lamp illumination conditions. In addition, it has been shown that NO_3· photolysis only occurs in visible light (Aldener et al., 2006). Therefore, the LED lamp setup was used in subsequent experiments to exclude the direct photolysis of both KNO_3 and NO_3·, but allow the excitation of TiO_2. This approach allowed us to investigate the process of photocatalytic renoxification caused by HCHO in the presence of photogenerated NO_3·.

Atmospheric trace gases can undergo photocatalytic reactions on the surface of TiO_2 (Chen et al., 2012). As the illumination time increased, the concentration of HCHO showed a linear downward trend, which was found to fit ~~consistent with~~ zero-order reaction kinetics (Figure S~~6~~7). The zero-order reaction rate constants of HCHO on TiO_2 and 4 wt.% KNO_3-TiO_2 particles were 9.1×10^{-3} and 1.4×10^{-2} ppm min^{-1}, respectively, which were much higher than that for gaseous HCHO photolysis (Shang et al., 2017). We suggested that the produced NO_3· contributed to the enhanced uptake of HCHO. ~~Therefore, we suggest that NO_3· production contributed to enhanced HCHO uptake.~~ In the following study, the effect of HCHO on the photocatalytic renoxification of NO_3^--TiO_2 was explored.~~Future studies should explore whether HCHO affects the photocatalytic renoxification of NO_3^--TiO_2.~~

Variation in NO_x concentration within the chamber containing nitrate-TiO_2 particles with or without HCHO is shown in Figure 2. For 4 wt.% KNO_3-TiO_2 particles, the NO_x concentration began to increase upon irradiation in the presence of HCHO, reaching ~3861 mmol-normalized ppb (equivalent to 110 ppb) ~~110 ppb~~ within 120 min. This result indicates that HCHO greatly promoted photocatalytic renoxification of KNO_3 on the surfaces of TiO_2 particles. This reaction process can be divided into two stages: a rapid increase within the first 60 min and a slower increase within the following 60 min, each consistent with zero-order reaction kinetics. The slow stage is due to the photodegradation of HCHO on KNO_3-TiO_2 aerosols, which led to a decrease in its concentration, gradually weakening the positive effect. NO_x is the sum of NO_2 and NO, both of which showed a two-stage concentration increase (Figure S8). The NO_2 generation rate was nearly 6 times that of NO, as compared to using the zero-order rate constant within 60 min (1.18 ppb min^{-1} NO_2, $R^2 = 0.96$; 0.19 ppb min^{-1} NO, $R^2 = 0.91$). This burst-like generation of NO_x can be ascribed to the reaction between generated NO_3· and HCHO via hydrogen abstraction to form adsorbed nitric acid (HNO_3(ads)) on TiO_2 particles. We measured the pH of water extracts in NO_3^--TiO_2 systems with and without HCHO. It was found that the pH decreased by 1.7% for KNO_3-TiO_2, suggesting the formation of acidic species such as HNO_3(ads) in this study. Based on the analysis of the absorption cross section of HNO_3 adsorbed on fused silica surface, the HNO_3(ads) absorption spectrum has been reported to be red-shifted compared to HNO_3(g), extending from 350 to 365 nm, with a simultaneous cross-sectional increase (Du and Zhu, 2011). Therefore, HNO_3(ads)

was subjected to photolysis to produce NO_2 and HONO (Eqs. (6)-(8)) under the LED lamp used in this study. A previous study of HNO_3 photolysis on the surface of Pyrex glass showed that the ratio of the formation rates of photolysis products ($J_{NOx}/J_{(NOx+HONO)}$) was > 97% at RH = 0% (Zhou et al., 2003), suggesting that NO_x is the main gaseous product under dry conditions. Thus, the effect of HONO on product distribution and NO_x concentration was negligible in this study. Together, these results suggest that $NO_3\cdot$ and HCHO generate HNO_3(ads) on particle surfaces through hydrogen abstraction, which contributes to the substantial release of NO_x via photolysis. This photocatalytic renoxification via the NO_3^--$NO_3\cdot$-HCHO-HNO_3-NO_x pathway is important considering the high abundance of hydrogen donor organics in the atmosphere.

$$NO_3\cdot + HCHO \rightarrow CHO\cdot + HNO_3(ads) \quad (5)$$

$$HNO_3(ads) + h\upsilon \rightarrow [HNO_3]^*(ads) \quad (6)$$

$$[HNO_3]^*(ads) \rightarrow HNO_2(ads) + O(^3P)(ads) \quad (7)$$

$$[HNO_3]^*(ads) \rightarrow NO_2(ads) + \cdot OH(ads) \quad (8)$$

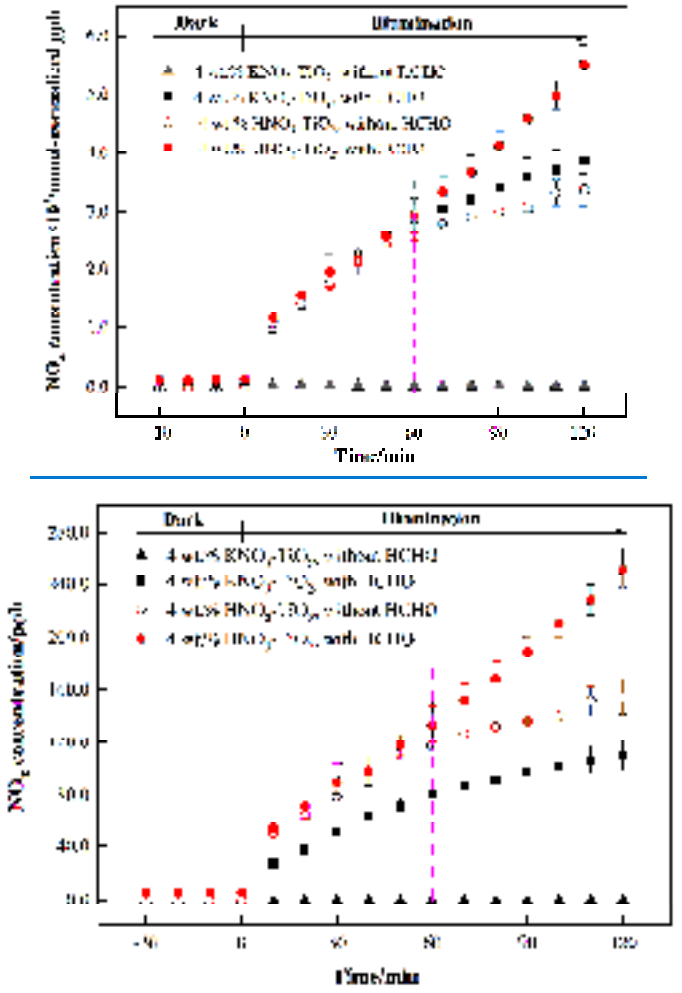

Figure 2. Effect of formaldehyde on the renoxification processes of different nitrate-doped particles at 293 K and 0.8% of relative humidity. 365 nm LED lamps were used during the illumination experiment. The initial concentration of HCHO was about 9 ppm.

To demonstrate the proposed HCHO mechanism and the photolysis contribution of HNO_3 to NO_x, we prepared an HNO_3-TiO_2 sample by directly dissolving TiO_2 into

dilute nitric acid. The formation of NO_x on HNO_3-TiO_2 without HCHO under illumination was obvious and at a rate comparable with ~~(Figure 2), and occurred even more rapidly than~~ that on KNO_3-TiO_2 with HCHO (Figure 2). The renoxification of HNO_3-TiO_2 particles was further enhanced following the introduction of HCHO. ~~The NO_x concentration increased by ~250 ppb after 2 h of illumination, which was 2.2 times faster than the increase in KNO_3-TiO_2 concentration under the same conditions.~~ This ~~is difference is due to the fact~~because that HNO_3 dissociates on particle surfaces to generate NO_3^-, such that HNO_3 exists on TiO_2 as both HNO_3(ads) and NO_3^-(ads). Similarly, NO_3^-(ads) completed the NO_3^--NO_3·-HCHO-HNO_3-NO_x pathway as described above through the reaction process shown in Eqs. (2) to (8). The rates of NO_x production from HNO_3-TiO_2 particles with and without HCHO were similar for the first 60 min (Figure 2), mainly due to the direct photolysis of partial HNO_3(ads). However, after 60 min, NO_x was generated rapidly in the presence of HCHO, perhaps due to the dominant photocatalytic renoxification of NO_3^-(ads). These findings indicate that HCHO converts NO_3^- on particle surfaces into HNO_3(ads) by reacting with NO_3·, and then HNO_3(ads) photolyzes at a faster rate to generate NO_x, allowing HCHO to enhance the formation of NO_x. Overall, the photocatalytic renoxification of NO_3^--TiO_2 particles affects atmospheric oxidation and the nitrogen cycle, and the presence of HCHO further enhances this impact.

Photocatalytic renoxification reaction occurs on the surfaces of mineral dust due to the presence of semiconductor oxides with photocatalytic activity such as TiO_2 (Ndour et al., 2009). In order to confirm this, we synthesized nitrate with inert SiO_2

as a comparison. It can be seen from Figure S9 that no NO_2 formation was observed whether HCHO was present or not, indicating that photocatalytically active particle TiO_2 is critical to the photocatalytic renoxification process. Furthermore, a kind of commercial mineral dust ATD was selected~~In this study, we selected the commercial mineral dust ATD~~ to study the effects of HCHO on this process. We detected ·OH in irradiated pure TiO_2 and ATD samples using electron spin resonance (ESR) technique, and found that for ATD samples, the peak intensity of ·OH generation was 40% that of TiO_2 samples (Figure S~~8~~10). ·OH originates in the reaction of h^+ with surface adsorbed water (Ahmed et al., 2014). ATD contains semiconductor oxides such as TiO_2 and Fe_2O_3, and is thought to exhibit photocatalytic properties affecting the renoxification of nitrate. The NO_3^- content of ATD is 4×10^{17} molecules m^{-2}, which is ~0.25 wt.% of the total mass (Huang et al., 2015; Jiyeon et al., 2017). The NO_x concentration changes observed in the environmental chamber demonstrated that HCHO promoted the renoxification of ATD particles (Figure S~~9~~11). This result suggests that mineral dust containing photocatalytic semiconductor oxides such as TiO_2, Fe_2O_3, and ZnO can greatly promote the conversion of granular nitrate to NO_x in the presence of HCHO.

3.3 Influential factors on the photocatalytic renoxification process

3.3.1 The influence of nitrate type

As discussed above, HNO_3 and KNO_3 undergo different renoxification processes on the surface of TiO_2 under the same illumination conditions, suggesting that cations

bound to NO_3^- significantly affect NO_x production. Different types of cations coexist with nitrate ions in atmospheric particulate matter, among which ammonium ions (NH_4^+) are important water-soluble ions that can be higher in content than K^+ in urban fine particulate matter (Zhou et al., 2016; Tang et al., 2021; Wang et al., 2021), especially in heavily polluted cities.(Tian et al., 2020) Equal amounts of 4 wt.% NH_4NO_3-TiO_2 particles were introduced into the chamber and illuminated under the same conditions. Similar as Figure 2, millimole normalized ppb was used in order to compare the amount of NO_x release for different kinds of nitrate with same percentage weight. It can be seen that HCHO had a much stronger positive effect on the release of NO_x over NH_4NO_3-TiO_2 particles (Figure 3), which may be ascribed to NH_4^+. Combined with the results of NH_4NO_3-TiO_2 and KNO_3-TiO_2 particles, it seems that the affinity rather than electrostatic repulsion should be the primary effect of cations on the production of NO_x. On substrates without photocatalytic activity such as SiO_2 and Al_2O_3, NH_4NO_3 cannot generate NO_x,(Ma et al., 2021) such that NO_x production depends on the effect of TiO_2. The h^+ generated by TiO_2 excitation reacts with adsorbed H_2O to produce ·OH (Eq. (9)), which gradually oxidizes NH_4^+ to NO_3^- (Eq. (10)). In our previous study, we demonstrated that irradiated $(NH_4)_2SO_4$-TiO_2 samples had lower NH_4^+ and NO_3^- peaks (Shang et al., 2017). Therefore, more NO_3^- participated in the photocatalytic renoxification process via the NO_3^--NO_3·-HCHO-HNO_3-NO_x pathway to generate NO_x. Moreover，the results without HCHO are shown in Figure ~~4a~~S12, both NH_4NO_3-TiO_2 particles and KNO_3-TiO_2 particles produced almost no NO_x, indicating the importance of HCHO

for renoxification to occur. Due to the high content of NH_4NO_3 in atmospheric particulate matter, the positive effect of HCHO on the photocatalytic renoxification process may have some impact on the concentrations of NO_x and other atmospheric oxidants.

$$h^+ + H_2O \rightarrow \cdot OH \quad (9)$$

$$\cdot OH + NH_4^+ / NH_3 \rightarrow NO_2^- \rightarrow NO_3^- \quad (10)$$

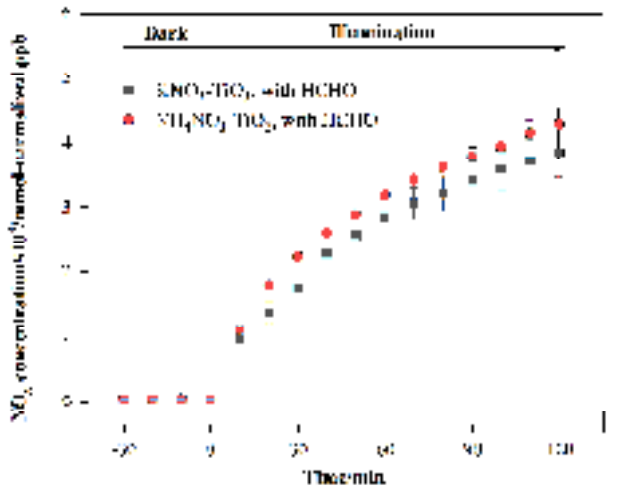

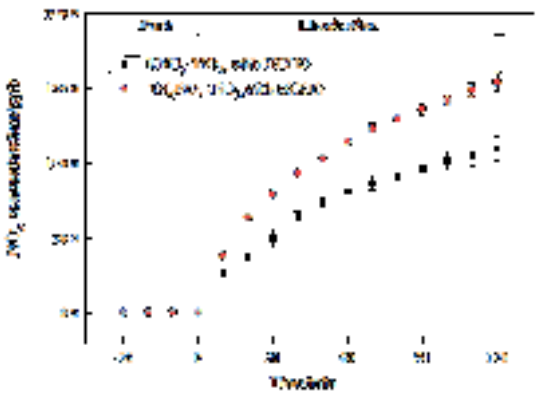

Figure 3. Effect of formaldehyde on the renoxification processes of 4 wt.%

401 NH_4NO_3-TiO_2 and 4 wt.% KNO_3-TiO_2 particles at 293 K and 0.8% of relative
402 humidity. 365 nm LED lamps were used during the irradiation experiment. The initial
403 concentration of HCHO was about 9 ppm.
404
405 **3.3.2 The influence of nitrate content**
406 Atmospheric particles have a wide range of nitrate content; differences in the relative
407 amounts of nitrate and TiO_2 in atmospheric particles may affect the renoxification
408 process. Therefore, we investigated the effects of nitrate concentration gradients on
409 renoxification. Changes in the NO_x concentrations of NO_3^--TiO_2 composite particles,
410 with or without HCHO, according to reaction time under 365 nm LED illumination
411 confirmed zero-order reaction kinetics. Therefore, we applied zero-order rate
412 constants to compare particles with different nitrate contents. For KNO_3-TiO_2, NO_x
413 was not generated in the absence of HCHO, even at high NO_3^- nitrate concentrations
414 (Figure 4a) because no photolysis of either NO_3^- or the NO_3 radical occurred under
415 365 nm LED illumination. For NH_4NO_3-TiO_2, the rate of NO_x generation increased in
416 the absence of HCHO as NH_4NO_3 content increased, and at higher levels (80 and 95
417 wt.%), the NO_x generation rate constant reached a plateau at ~ 8.0×10^{-2} ppb min^{-1}
418 because both NH_4^+ and NO are photochemically oxidized on TiO_2 to generate NO_3^-,
419 and part of this NO was oxidized to NO_2 by O_2.(Ma et al., 2021) Higher NO_3^- content
420 leads to higher NH_4^+ concentration; thus, more NH_4^+ participated in the generation of
421 NO_x through photooxidation. When NO_3^- content reached 80 wt.% or higher, limited
422 TiO_2 content in the chamber led to the saturation of NH_4^+ photooxidation, preventing

~~further NO_x generation. NO_x release rates over NO_3^--TiO_2 as nitrate content increased in the presence of HCHO are shown in Figure 4b. The NO_x production rate first increased and then decreased, with a maximum of 4 wt.% nitrate content among both KNO_3-TiO_2 and NH_4NO_3-TiO_2 particles. This increasing trend was caused by the increased opportunities for contact between TiO_2 and NO_3^- as nitrate content increased, which facilitated the combination of h^+ with NO_3^- to form NO_3·. The trend began to decrease when nitrate content exceeded 4 wt.%. Higher NO_3^- content hindered reactions on the surface of TiO_2, but rapidly decreased the Brunauer, Emmett and Teller (BET) surface area of the composite particles (Shang et al., 2017), which weakened HCHO uptake and particle surface reactions. The amount of NO_x produced by NH_4NO_3-TiO_2 was consistently higher than that of KNO_3-TiO_2. The possible reasons for this difference are as follows. First, like the K^+ blocking effect discussed in section 3.1, NO_3· generated from the reaction of NO_3^- with h^+ was weakened; thus, little adsorbed HNO_3 was available for further renoxification. Additionally, NH_4^+ can undergo a photooxidation reaction to generate more NO_x by TiO_2, as occurs in the absence of HCHO.~~

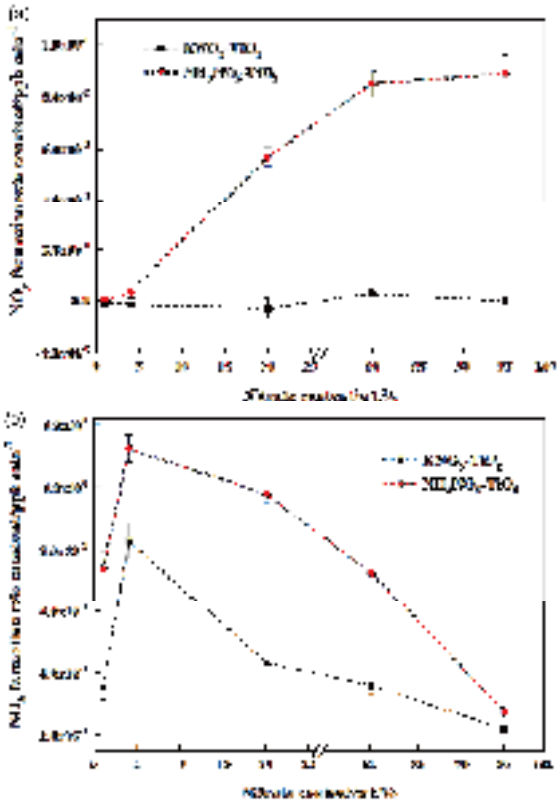

~~Figure 4.~~ ~~Effect of nitrate content (1 wt.%, 4 wt.%, 20 wt.%, 80 wt.% and 95 wt.%) on the release of NO_x for NH_4NO_3-TiO_2 and KNO_3-TiO_2 at 293 K and 0.8% of relative humidity. 365 nm LED lamps were used during the illumination experiment. (a) without HCHO; (b) the initial concentration of HCHO was about 9 ppm.~~

3.3.2~~3~~ The influence of relative humidity

Water on particle surfaces can participate directly in the heterogeneous reaction process. As shown in Eq. (9), H_2O ~~is~~can be captured by h^+ to generate ·OH with strong oxidizability in photocatalytic reactions. The first-order photolysis rate constant of NO_3^- on TiO_2 particles decreases by an order of magnitude, from (5.7 ±

Formatted: Indent: First line: 2 ch

449 0.1) × 10^{-4} s^{-1} on dry surfaces to (7.1 ± 0.8) × 10^{-5} s^{-1} when nitrate is coadsorbed
450 with water above monolayer coverage (Ostaszewski et al., 2018). We explored the
451 positive effect of HCHO on the NO_3^--TiO_2 particle photocatalytic renoxification at
452 different RH levels; the results are shown in Figure ~~5~~4a. For KNO_3-TiO_2 particles, the
453 rate of NO_x production decreased as the RH of the environmental chamber increased,
454 indicating that increased water content in the gas phase hindered photocatalytic
455 renoxification for two reasions: H_2O competes with NO_3^- for h^+ on the surface of
456 TiO_2 to generate ·OH, reducing the generation of NO_3·, and competitive adsorption
457 between H_2O and HCHO causes the generated ·OH to compete with NO_3· for HCHO,
458 hindering the formation of HNO_3(ads) on particle surfaces. Moreover, it is also
459 possible that the loss of NO_x on the wall increases under high humidity conditions,
460 resulting in a decrease in its concentration. This competitive process also occurs on
461 the surface of NH_4NO_3-TiO_2 particles, but at RH = 70%, the NO_x generation rate
462 constant is slightly higher. The deliquescent humidity of NH_4NO_3 at 298 K is ~62%,
463 such that NH_4NO_3 had already deliquesced at RH = 70%, forming an
464 NH_4^+/NH_3-NO_3^- liquid system on the particle surfaces. This quasi-liquid phase
465 improved the dispersion of TiO_2 in NH_4NO_3, resulting in greater NO_x release. The
466 deliquescent humidity of KNO_3-TiO_2 was > 90%,(2009) such that no phase change
467 occurred at RH = 70%, and the renoxification reaction rate retained a downward trend.
468 In the presence of H_2O, in addition to the NO_3^--NO_3·-HCHO-HNO_3 pathway
469 observed in this study, there are a variety of HNO_3 generation paths, such as the
470 hydrolysis of N_2O_5 via the NO_2-N_2O_5-HNO_3 pathway (Brown et al., 2005), the

oxidation of NO_2 by ·OH (Burkholder et al., 1993), and the reaction of NO_3· with H_2O (Schutze and Herrmann, 2005), all of which require further consideration and study.

The formation rates of NO and NO_2 are shown in Figure ~~5~~4b and c, respectively. NO_2 was the main product of surface HNO_3 photolysis. Under humid conditions, generated NO_2(ads) continued to react with H_2O adsorbed on the surface to form HONO(ads). HONO was desorbed from the surface and released into the gas phase (Zhou et al., 2003; Bao et al., 2018; Pandit et al., 2021), providing gaseous HONO to the reaction system. Because the NO_x concentration remained high, the effect of HONO on NO_x analyzer results was negligible (Shi et al., 2021). As NO_2 can form NO_2^- with e^-, a reverse reaction also occurred between NO_2^- and HONO in the presence of H_2O (Ma et al., 2021; Garcia et al., 2021). Therefore, the increase in H_2O increased the proportion of HONO in the nitrogen-containing products, such that the NO_x generation rate decreased as RH increased. Comparing Figure ~~5~~4b and c shows that, as RH increased, the NO production rate constant decreased more than that of NO_2. HONO and NO_2 generated by the photolysis of HNO_3(ads) decreased accordingly, i.e., the NO source decreased. However, generated NO_2 and NO underwent photocatalytic oxidation on the surface of TiO_2, and NO photodegradation was more significant under the same conditions (Hot et al., 2017). Generally, a certain amount of HONO will be generated during the reaction between HCHO and NO_3^--TiO_2 particles when RH is high, which affects the concentrations of atmospheric ·OH, NO_x, and O_3. This process is more likely to occur in summer due to

high RH and light intensity affecting atmospheric oxidation. In drier winters or dusty weather, when TiO_2 content is high, HCHO greatly promotes the photocatalytic renoxification of NO_3^--TiO_2 particles, thereby releasing more NO_x into the atmosphere, affecting the global atmospheric nitrogen budget. Thus, regardless of the seasonal and regional changes, renoxification has significant practical importance.

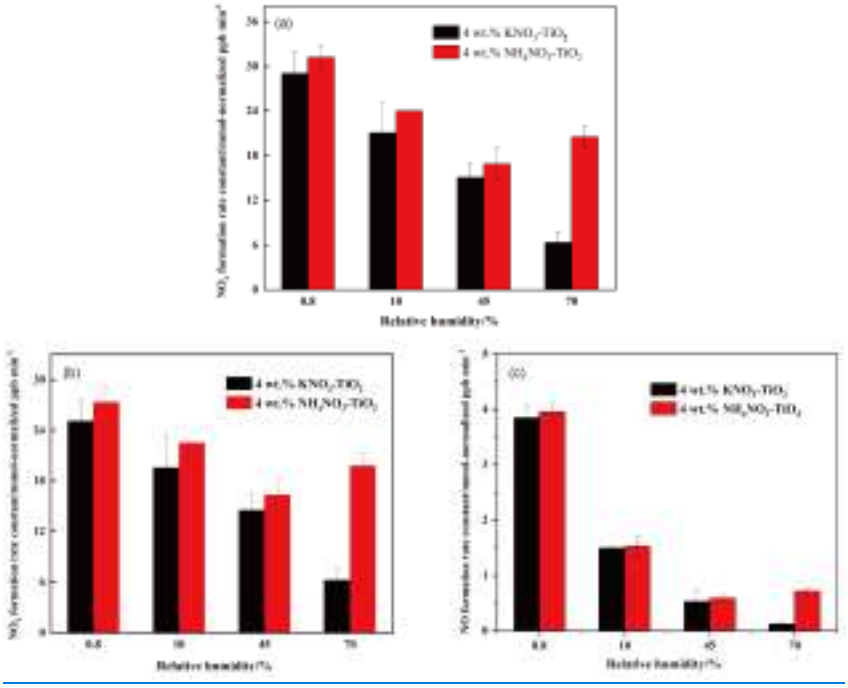

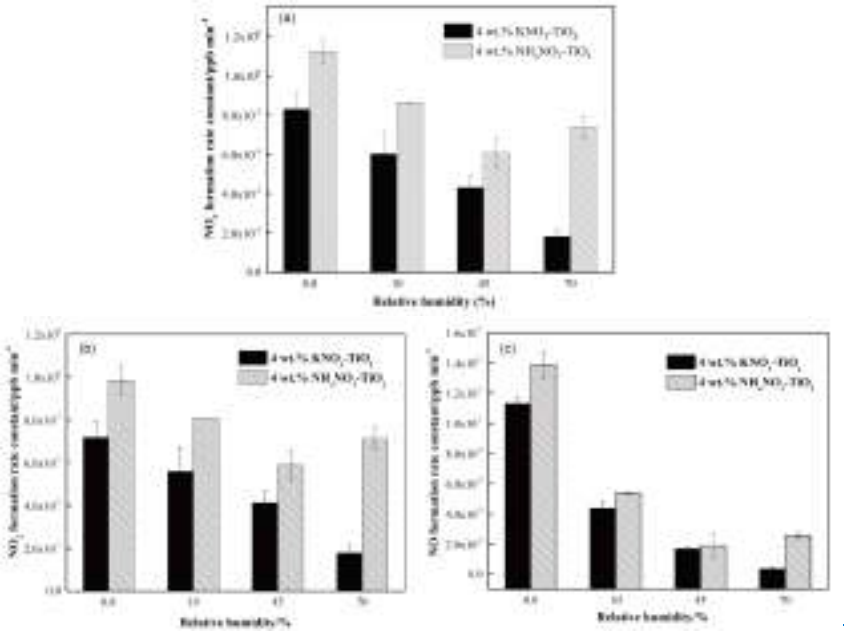

Figure ~~S4~~4. Effect of relative humidity on the release of NO_x (a), NO_2 (b), NO (c) over 4 wt.% NH_4NO_3-TiO_2 and 4 wt.% KNO_3-TiO_2 particles at 293 K. 365 nm LED lamps were used during the illumination experiment. The initial concentration of HCHO was about 9 ppm.

3.3.~~4~~3 The influence of initial HCHO concentration

To explore whether HCHO promotes nitrate renoxification at natural concentration levels, we reduced the initial concentration of HCHO in the environmental chamber by a factor of 10, to ~1.0 ppm. The positive effect of HCHO on the photocatalytic renoxification of KNO_3-TiO_2 particles was clearly weakened, with NO_2 concentration first increasing and then decreasing, and NO concentration remaining stable (Figure S1~~0~~3). The HCHO concentration decreased due to its consumption during the reaction, making its positive effect decline quickly. The

photocatalytic oxidation reaction between NO_x and photogenerated reactive oxygen species (ROS) on the TiO_2 surface further decreased the NO_x concentration. Photocatalytic oxidation of NO_x by ROS on TiO_2 particles occurred at an HCHO concentration of 9 ppm, but the positive effect of HCHO remained dominant. Thus, no decrease in NO_x concentration was observed within 120 min in our experiments.

The concentration of HCHO in the atmosphere is relatively low, with a balance between the photocatalytic oxidation decay of NO_x and the release of NO_x via photocatalytic renoxification. The mutual transformation between particulate NO_3^- and gaseous NO_x is more complex. The effect of low-concentration HCHO on the renoxification of NO_3^--TiO_2 particles requires further investigation. However, many types of organics provide hydrogen atoms in the atmosphere, including alkanes (e.g., methane and n-hexane), aldehydes (e.g., acetaldehyde), alcohols (e.g., methanol and ethanol), and aromatic compounds (e.g., phenol) that react with $NO_3\cdot$ to produce nitric acid (Atkinson, 1991). These organics, together with HCHO, play similar positive roles in photocatalytic renoxification and, therefore, influence NO_x concentrations.

4 Atmospheric implications

Nitric acid and nitrate are not only the final sink of NO_x in the atmosphere but are also among its important sources. NO_x from nitrate through renoxification is easily overlooked. The renoxification of nitrate on the surface of TiO_2 particles can be divided into photolytic renoxification and photocatalytic renoxification. The

photocatalytic performance of TiO_2 promotes the renoxification process, which explains the influence of semiconducting metal oxide components on atmospheric mineral particles during the renoxification of nitrate. Although most previous studies have focused on solid-phase nitrate renoxification, our exploration of the roles of HCHO in this study will allow us to examine complex real-world pollution scenarios, in which multiple atmospheric pollutants coexist, as well as the effects of organic pollutants on the renoxification process. Atmospheric HCHO is taken up at the surface of particulate matter, accounting for up to ~50% of its absorption (Li et al., 2014), such that the heterogeneous participation of HCHO during renoxification is important. This study is the first to report that HCHO has a positive effect on the photocatalytic renoxification of nitrate on TiO_2 particles, via the NO_3^--NO_3·-HCHO-HNO_3-NO_x pathway (Figure ~~6~~5), further increasing the release of NO_x and other nitrogen-containing active species, which in turn affects the photochemical cycle of HO_x radicals in the atmosphere and the formation of important atmospheric oxidants such as O_3. Although in the case of high concentrations of HCHO in our experiment, the response to the real situation will be biased, the results of this study illustrate a possible way of HCHO in influencing nitrate renoxification in the atmosphere. Factors such as particulate matter composition, RH, and initial HCHO concentration all influence the positive effect of HCHO; notably, H_2O competes with NO_3^- for photogenerated holes. Based on these findings, two balance systems should be explored in depth: the influence of RH on the generation rates of HONO and NO_x, as water increases the proportion of HONO in

556 nitrogen-containing products; and the balance between the photocatalytic degradation
557 of generated NO_x on TiO_2 particles and the positive effect of HCHO on NO_x
558 generation at low HCHO concentrations.

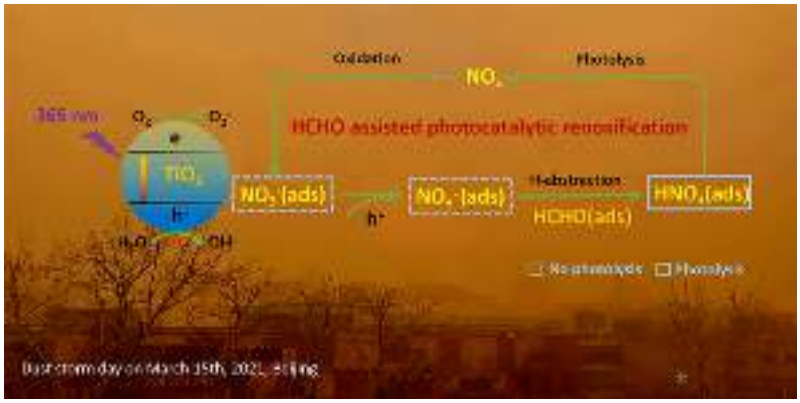

559

560 **Figure 65.** Positive role of HCHO on the photocatalytic renoxification of nitrate-TiO_2
561 composite particles via the NO_3^--NO_3·-HCHO-HNO_3-NO_x pathway.

562 Based on our results, we conclude that in photochemical processes on the
563 surfaces of particles containing semiconductor oxides, with the participation of
564 hydrogen donor organics, a significant synergistic photocatalytic renoxification
565 enhancement effect alters the composition of surface nitrogenous species via the
566 NO_3^--NO_3·-hydrogen donor-HNO_3-NO_x pathway, thereby affecting atmospheric
567 oxidation and nitrogen cycling. The positive effect of HCHO can be extended from
568 TiO_2 in this study to other components of mineral dust such as Fe_2O_3 and ZnO with
569 photocatalytic activity, which may have practical applications. Our proposed reaction
570 mechanism by which HCHO promotes photocatalytic renoxification will improve
571 existing atmospheric chemistry models and reduce discrepancies between model
572 simulations and field observations.

Supplement.

Detailed information of Figures S1-1~~0~~3 (which include the spectra of the lamps, DRIFTS spectra of KNO_3-TiO_2 particles, size distribution of KNO_3-TiO_2 ~~TiO_2~~ particles, ~~and~~ changes of HCHO concentration in ~~environmental~~the chamber, changes of NO_x concentration under different reaction conditions, photodegradation curves of HCHO, ESR spectra of TiO_2 and ATD particles), and Table S1 (which demonstrates ATD chemical composition) .

Formatted: Font color: Red

Formatted: Font color: Red

Formatted: Indent: First line: 0 ch

Acknowledgments

The authors are grateful to the financial support provided by National Natural Science Foundation of China (Nos. 41961134034, 21876003, ~~41961134034~~ and 21277004), the Second Tibetan Plateau Scientific Expedition and Research (No. 2019QZKK0607)~~, and the 111 Project Urban Air Pollution and Health Effects (B20009)~~.

References

Aghazadeh, M.: Preparation of Gd_2O_3 Ultrafine Nanoparticles by Pulse Electrodeposition Followed by Heat-treatment Method, Journal of Ultrafine Grained and Nanostructured Materials, 49, 80-86, 10.7508/jufgnsm.2016.02.04, 2016.

Ahmed, A. Y., Kandiel, T. A., Ivanova, I., and Bahnemann, D.: Photocatalytic and photoelectrochemical oxidation mechanisms of methanol on TiO_2 in aqueous solution, Applied Surface Science, 319, 44-49, 10.1016/j.apsusc.2014.07.134, 2014.

Aldener, M., Brown, S. S., Stark, H., Williams, E. J., Lerner, B. M., Kuster, W. C., Goldan, P. D., Quinn, P. K., Bates, T. S., Fehsenfeld, F. C., and Ravishankara, A. R.: Reactivity and loss mechanisms of NO_3 and N_2O_5 in a polluted marine environment: Results from in situ measurements during New England Air Quality Study 2002, Journal of Geophysical Research-Atmospheres, 111, D23S73, 10.1029/2006jd007252, 2006.

Alexander, B., Sherwen, T., Holmes, C. D., Fisher, J. A., Chen, Q., Evans, M. J., and Kasibhatla, P.: Global inorganic nitrate production mechanisms: comparison of a global model with nitrate isotope observations, Atmospheric Chemistry and Physics, 20, 3859-3877, 10.5194/acp-20-3859-2020, 2020.

Atkinson, R.: Kinetics and mechanisms of the gas-phase reactions of the NO_3 radical with organic-comounds, Journal of Physical and Chemical Reference Data, 20, 459-507, 10.1063/1.555887, 1991.

Baergen, A. M. and Donaldson, D. J.: Photochemical Renoxification of Nitric Acid on Real Urban Grime, Environmental Science & Technology, 47, 815-820, 10.1021/es3037862, 2013.

Bao, F., Li, M., Zhang, Y., Chen, C., and Zhao, J.: Photochemical Aging of Beijing Urban $PM_{2.5}$: HONO Production, Environmental Science & Technology, 52, 6309-6316, 10.1021/acs.est.8b00538, 2018.

Bao, F., Jiang, H., Zhang, Y., Li, M., Ye, C., Wang, W., Ge, M., Chen, C., and Zhao, J.: The Key Role of Sulfate in the Photochemical Renoxification on Real $PM_{2.5}$, Environmental Science & Technology, 54, 3121-3128, 10.1021/acs.est.9b06764, 2020.

Bedjanian, Y. and El Zein, A.: Interaction of NO_2 with TiO_2 Surface Under UV Irradiation: Products Study, Journal of Physical Chemistry A, 116, 1758-1764, 10.1021/jp210078b, 2012.

Brown, S. S., Osthoff, H. D., Stark, H., Dube, W. P., Ryerson, T. B., Warneke, C., de Gouw, J. A., Wollny, A. G., Parrish, D. D., Fehsenfeld, F. C., and Ravishankara, A. R.: Aircraft observations of daytime NO_3 and N_2O_5 and their implications for tropospheric chemistry, Journal of Photochemistry and Photobiology a-Chemistry,

176, 270-278, 10.1016/j.jphotochem.2005.10.004, 2005.

Burkholder, J. B., Talukdar, R. K., Ravishankara, A. R., and Solomon, S.: Temperature-dependence of the HNO_3 UV absorption cross-sections, Journal of Geophysical Research-Atmospheres, 98, 22937-22948, 10.1029/93jd02178, 1993.

Chen, H., Nanayakkara, C. E., and Grassian, V. H.: Titanium Dioxide Photocatalysis in Atmospheric Chemistry, Chemical Reviews, 112, 5919-5948, 10.1021/cr3002092, 2012.

Deng, J. J., Wang, T. J., Liu, L., and Jiang, F.: Modeling heterogeneous chemical processes on aerosol surface, Particuology, 8, 308-318, 10.1016/j.partic.2009.12.003, 2010.

Dentener, F. J. and Crutzen, P. J.: Reaction of N_2O_5 on tropospheric aerosols-impact on the global distributions od NO_x, O_3, and OH, Journal of Geophysical Research-Atmospheres, 98, 7149-7163, 10.1029/92jd02979, 1993.

Du, J. and Zhu, L.: Quantification of the absorption cross sections of surface-adsorbed nitric acid in the 335-365 nm region by Brewster angle cavity ring-down spectroscopy, Chemical Physics Letters, 511, 213-218, 10.1016/j.cplett.2011.06.062, 2011.

Finlayson-Pitts, B. J. and Pitts, J. J. N.: Chemistry of the Upper and Lower Atmosphere: Theory, Experiments and Applications, 10.1023/A:1024719803484, Academic Press1999.

Garcia, S. L. M., Pandit, S., Navea, J. G., and Grassian, V. H.: Nitrous Acid (HONO) Formation from the Irradiation of Aqueous Nitrate Solutions in the Presence of Marine Chromophoric Dissolved Organic Matter: Comparison to Other Organic Photosensitizers, Acs Earth and Space Chemistry, 5, 3056-3064, 10.1021/acsearthspacechem.1c00292, 2021.

George, C., Ammann, M., D'Anna, B., Donaldson, D. J., and Nizkorodov, S. A.: Heterogeneous Photochemistry in the Atmosphere, Chemical Reviews, 115, 4218-4258, 10.1021/cr500648z, 2015.

Goodman, A. L., Bernard, E. T., and Grassian, V. H.: Spectroscopic study of nitric acid and water adsorption on oxide particles: Enhanced nitric acid uptake kinetics in the presence of adsorbed water, Journal of Physical Chemistry A, 105, 6443-6457,

10.1021/jp0037221, 2001.

Harris, G. W., Carter, W. P. L., Winer, A. M., Pitts, J. N., Platt, U., and Perner, D.: Observations of nitrous-acid in the los-angeles atmosphere and implications for predictions of ozone precursor relationships, Environmental Science & Technology, 16, 414-419, 10.1021/es00101a009, 1982.

Hot, J., Martinez, T., Wayser, B., Ringot, E., and Bertron, A.: Photocatalytic degradation of NO/NO_2 gas injected into a 10 m^3 experimental chamber, Environmental Science and Pollution Research, 24, 12562-12570, 10.1007/s11356-016-7701-2, 2017.

Huang, L., Zhao, Y., Li, H., and Chen, Z.: Kinetics of Heterogeneous Reaction of Sulfur Dioxide on Authentic Mineral Dust: Effects of Relative Humidity and Hydrogen Peroxide, Environmental Science & Technology, 49, 10797-10805, 10.1021/acs.est.5b03930, 2015.

Jiyeon, Park, Myoseon, Jang, Zechen, and Yu: Heterogeneous Photo-oxidation of SO_2 in the Presence of Two Different Mineral Dust Particles: Gobi and Arizona Dust, Environmental Science & Technology, 51, 9605-9613, 10.1021/acs.est.7b00588, 2017.

Kasibhatla, P., Sherwen, T., Evans, M. J., Carpenter, L. J., Reed, C., Alexander, B., Chen, Q., Sulprizio, M. P., Lee, J. D., Read, K. A., Bloss, W., Crilley, L. R., Keene, W. C., Pszenny, A. A. P., and Hodzic, A.: Global impact of nitrate photolysis in sea-salt aerosol on NOx, OH, and O_3 in the marine boundary layer, Atmospheric Chemistry and Physics, 18, 11185-11203, 10.5194/acp-18-11185-2018, 2018.

Kim, W.-H., Song, J.-M., Ko, H.-J., Kim, J. S., Lee, J. H., and Kang, C.-H.: Comparison of Chemical Compositions of Size-segregated Atmospheric Aerosols between Asian Dust and Non-Asian Dust Periods at Background Area of Korea, Bulletin of the Korean Chemical Society, 33, 3651-3656, 10.5012/bkcs.2012.33.11.3651, 2012.

Lee, J. D., Moller, S. J., Read, K. A., Lewis, A. C., Mendes, L., and Carpenter, L. J.: Year-round measurements of nitrogen oxides and ozone in the tropical North Atlantic marine boundary layer, Journal of Geophysical Research-Atmospheres, 114, D21302,

687 10.1029/2009jd011878, 2009.
688 Lesko, D. M. B., Coddens, E. M., Swomley, H. D., Welch, R. M., Borgatta, J., and
689 Navea, J. G.: Photochemistry of nitrate chemisorbed on various metal oxide surfaces,
690 Physical Chemistry Chemical Physics, 17, 20775-20785, 10.1039/c5cp02903a, 2015.
691 Li, L., Wang, Q., Zhang, X., She, Y., Zhou, J., Chen, Y., Wang, P., Liu, S., Zhang, T.,
692 Dai, W., Han, Y., and Cao, J.: Characteristics of single atmospheric particles in a
693 heavily polluted urban area of China: size distributions and mixing states,
694 Environmental Science and Pollution Research, 26, 11730-11742,
695 10.1007/s11356-019-04579-3, 2019.
696 Li, X., Rohrer, F., Brauers, T., Hofzumahaus, A., Lu, K., Shao, M., Zhang, Y. H., and
697 Wahner, A.: Modeling of HCHO and CHOCHO at a semi-rural site in southern China
698 during the PRIDE-PRD2006 campaign, Atmospheric Chemistry and Physics, 14,
699 12291-12305, 10.5194/acp-14-12291-2014, 2014.
700 Linsebigler, A. L., Lu, G. Q., and Yates, J. T.: Photocatalysis on TiO_2
701 surfaces-principles, mechanisms, and selected results, Chemical Reviews, 95,
702 735-758, 10.1021/cr00035a013, 1995.
703 Ma, Q., Zhong, C., Ma, J., Ye, C., Zhao, Y., Liu, Y., Zhang, P., Chen, T., Liu, C., Chu,
704 B., and He, H.: Comprehensive Study about the Photolysis of Nitrates on Mineral
705 Oxides, Environmental Science & Technology, 55, 8604-8612,
706 10.1021/acs.est.1c02182, 2021.
707 Maeda, N., Urakawa, A., Sharma, R., and Baiker, A.: Influence of Ba precursor on
708 structural and catalytic properties of Pt-Ba/alumina NO_x storage-reduction catalyst,
709 Applied Catalysis B-Environmental, 103, 154-162, 10.1016/j.apcatb.2011.01.022,
710 2011.
711 Monge, M. E., D"Anna, B., and George, C.: Nitrogen dioxide removal and nitrous
712 acid formation on titanium oxide surfaces--an air quality remediation process?,
713 Physical Chemistry Chemical Physics, 12, 8991-8998, 10.1039/b925785c, 2010.
714 Ndour, M., Conchon, P., D'Anna, B., Ka, O., and George, C.: Photochemistry of
715 mineral dust surface as a potential atmospheric renoxification process, Geophysical
716 Research Letters, 36, 4, 10.1029/2008gl036662, 2009.

717 Ninneman, M., Lu, S., Zhou, X. L., and Schwab, J.: On the Importance of
718 Surface-Enhanced Renoxification as an Oxides of Nitrogen Source in Rural and
719 Urban New York State, Acs Earth and Space Chemistry, 4, 1985-1992,
720 10.1021/acsearthspacechem.0c00185, 2020.
721 Ostaszewski, C. J., Stuart, N. M., Lesko, D. M. B., Kim, D., Lueckheide, M. J., and
722 Navea, J. G.: Effects of Coadsorbed Water on the Heterogeneous Photochemistry of
723 Nitrates Adsorbed on TiO_2, Journal of Physical Chemistry A, 122, 6360-6371,
724 10.1021/acs.jpca.8b04979, 2018.
725 Pandit, S., Garcia, S. L. M., and Grassian, V. H.: HONO Production from Gypsum
726 Surfaces Following Exposure to NO_2 and HNO_3: Roles of Relative Humidity and
727 Light Source, Environmental Science & Technology, 55, 9761-9772,
728 10.1021/acs.est.1c01359, 2021.
729 Platt, U., Perner, D., Harris, G. W., Winer, A. M., and Pitts, J. N.: Observations of
730 nitrous-acid in an urban atmosphere by differential optical-absorption, Nature, 285,
731 312-314, 10.1038/285312a0, 1980.
732 Read, K. A., Mahajan, A. S., Carpenter, L. J., Evans, M. J., Faria, B. V. E., Heard, D.
733 E., Hopkins, J. R., Lee, J. D., Moller, S. J., Lewis, A. C., Mendes, L., McQuaid, J. B.,
734 Oetjen, H., Saiz-Lopez, A., Pilling, M. J., and Plane, J. M. C.: Extensive
735 halogen-mediated ozone destruction over the tropical Atlantic Ocean, Nature, 453,
736 1232-1235, 10.1038/nature07035, 2008.
737 Reed, C., Evans, M. J., Crilley, L. R., Bloss, W. J., Sherwen, T., Read, K. A., Lee, J.
738 D., and Carpenter, L. J.: Evidence for renoxification in the tropical marine boundary
739 layer, Atmospheric Chemistry and Physics, 17, 4081-4092,
740 10.5194/acp-17-4081-2017, 2017.
741 Romer, P. S., Wooldridge, P. J., Crounse, J. D., Kim, M. J., Wennberg, P. O., Dibb, J.
742 E., Scheuer, E., Blake, D. R., Meinardi, S., Brosius, A. L., Thames, A. B., Miller, D.
743 O., Brune, W. H., Hall, S. R., Ryerson, T. B., and Cohen, R. C.: Constraints on
744 Aerosol Nitrate Photolysis as a Potential Source of HONO and NOx, Environmental
745 Science & Technology, 52, 13738-13746, 10.1021/acs.est.8b03861, 2018.
746 Rosseler, O., Sleiman, M., Nahuel Montesinos, V., Shavorskiy, A., Keller, V., Keller,

747 N., Litter, M. I., Bluhm, H., Salmeron, M., and Destaillats, H.: Chemistry of NOx on
748 TiO_2 Surfaces Studied by Ambient Pressure XPS: Products, Effect of UV Irradiation,
749 Water, and Coadsorbed K+, Journal of Physical Chemistry Letters, 4, 536-541,
750 10.1021/jz302119g, 2013.
751 Schuttlefield, J., Rubasinghege, G., El-Maazawi, M., Bone, J., and Grassian, V. H.:
752 Photochemistry of adsorbed nitrate, Journal of the American Chemical Society, 130,
753 12210-12211, 10.1021/ja802342m, 2008.
754 Schutze, M. and Herrmann, H.: Uptake of the NO_3 radical on aqueous surfaces,
755 Journal of Atmospheric Chemistry, 52, 1-18, 10.1007/s10874-005-6153-8, 2005.
756 Schwartz-Narbonne, H., Jones, S. H., and Donaldson, D. J.: Indoor Lighting Releases
757 Gas Phase Nitrogen Oxides from Indoor Painted Surfaces, Environmental Science &
758 Technology Letters, 6, 92-97, 10.1021/acs.estlett.8b00685, 2019.
759 Seltzer, K. M., Vizuete, W., and Henderson, B. H.: Evaluation of updated nitric acid
760 chemistry on ozone precursors and radiative effects, Atmospheric Chemistry and
761 Physics, 15, 5973-5986, 10.5194/acp-15-5973-2015, 2015.
762 Shang, J., Xu, W. W., Ye, C. X., George, C., and Zhu, T.: Synergistic effect of
763 nitrate-doped TiO_2 aerosols on the fast photochemical oxidation of formaldehyde,
764 Scientific Reports, 7, 1161, 10.1038/s41598-017-01396-x, 2017.
765 Shi, Q., Tao, Y., Krechmer, J. E., Heald, C. L., Murphy, J. G., Kroll, J. H., and Ye, Q.:
766 Laboratory Investigation of Renoxification from the Photolysis of Inorganic
767 Particulate Nitrate, Environmental science & technology, 55, 854-861,
768 10.1021/acs.est.0c06049, 2021.
769 Stemmler, K., Ammann, M., Donders, C., Kleffmann, J., and George, C.:
770 Photosensitized reduction of nitrogen dioxide on humic acid as a source of nitrous
771 acid, Nature, 440, 195-198, 10.1038/nature04603, 2006.
772 Sun, Y. L., Zhuang, G. S., Wang, Y., Zhao, X. J., Li, J., Wang, Z. F., and An, Z. S.:
773 Chemical composition of dust storms in Beijing and implications for the mixing of
774 mineral aerosol with pollution aerosol on the pathway, Journal of Geophysical
775 Research-Atmospheres, 110, D24209, 10.1029/2005jd006054, 2005.
776 Tang, M., Liu, Y., He, J., Wang, Z., Wu, Z., and Ji, D.: In situ continuous hourly

observations of wintertime nitrate, sulfate and ammonium in a megacity in the North China plain from 2014 to 2019: Temporal variation, chemical formation and regional transport, Chemosphere, 262, 10.1016/j.chemosphere.2020.127745, 2021.

Tian, S. S., Liu, Y. Y., Wang, J., Wang, J., Hou, L. J., Lv, B., Wang, X. H., Zhao, X. Y., Yang, W., Geng, C. M., Han, B., and Bai, Z. P.: Chemical Compositions and Source Analysis of $PM_{2.5}$ during Autumn and Winter in a Heavily Polluted City in China, Atmosphere, 11, 19, 10.3390/atmos11040336, 2020.

Verbruggen, S. W.: TiO_2 photocatalysis for the degradation of pollutants in gas phase: From morphological design to plasmonic enhancement, Journal of Photochemistry and Photobiology C-Photochemistry Reviews, 24, 64-82, 10.1016/j.jphotochemrev.2015.07.001, 2015.

Wang, H., Miao, Q., Shen, L., Yang, Q., Wu, Y., Wei, H., Yin, Y., Zhao, T., Zhu, B., and Lu, W.: Characterization of the aerosol chemical composition during the COVID-19 lockdown period in Suzhou in the Yangtze River Delta, China, Journal of environmental sciences (China), 102, 110-122, 10.1016/j.jes.2020.09.019, 2021.

Wang, Z., Ma, Y., Zheng, J., Li, S., Wang, L., and Zhang, Y.: Source apportionment of aerosols in urban Nanjing based on particle size distribution, Huanjing Huaxue-Environmental Chemistry, 34, 1619-1626, 10.7524/j.issn.0254-6108.2015.09.2015020303, 2015.

Wayne, R. P., Barnes, I., Biggs, P., Burrows, J. P., Canosamas, C. E., Hjorth, J., Lebras, G., Moortgat, G. K., Perner, D., Poulet, G., Restelli, G., and Sidebottom, H.: The nitrate radical-physics, chemistry, and the atmosphere, Atmospheric Environment Part a-General Topics, 25, 1-203, 10.1016/0960-1686(91)90192-a, 1991.

Ye, C., Gao, H., Zhang, N., and Zhou, X.: Photolysis of Nitric Acid and Nitrate on Natural and Artificial Surfaces, Environmental Science & Technology, 50, 3530-3536, 10.1021/acs.est.5b05032, 2016a.

Ye, C., Zhang, N., Gao, H., and Zhou, X.: Photolysis of Particulate Nitrate as a Source of HONO and NOx, Environmental Science & Technology, 51, 6849-6856, 10.1021/acs.est.7b00387, 2017.

Ye, C., Zhou, X., Pu, D., Stutz, J., Festa, J., Spolaor, M., Tsai, C., Cantrell, C.,

Mauldin, R. L., III, Campos, T., Weinheimer, A., Hornbrook, R. S., Apel, E. C., Guenther, A., Kaser, L., Yuan, B., Karl, T., Haggerty, J., Hall, S., Ullmann, K., Smith, J. N., Ortega, J., and Knote, C.: Rapid cycling of reactive nitrogen in the marine boundary layer, Nature, 532, 489-491, 10.1038/nature17195, 2016b.

Zhou, J. B., Xing, Z. Y., Deng, J. J., and Du, K.: Characterizing and sourcing ambient $PM_{2.5}$ over key emission regions in China I: Water-soluble ions and carbonaceous fractions, Atmospheric Environment, 135, 20-30, 10.1016/j.atmosenv.2016.03.054, 2016.

Zhou, X. L., Gao, H. L., He, Y., Huang, G., Bertman, S. B., Civerolo, K., and Schwab, J.: Nitric acid photolysis on surfaces in low-NOx environments: Significant atmospheric implications, Geophysical Research Letters, 30, 2217, 10.1029/2003gl018620, 2003.

Formatted: Justified

Supplement of

The Positive Effect of Formaldehyde on the Photocatalytic Renoxification of Nitrate on TiO_2 Particles

Yuhan Liu, Xuejiao Wang, Mengshuang Sheng, Chunxiang Ye, Jing Shang*

State Key Joint Laboratory of Environmental Simulation and Pollution Control, College of Environmental Sciences and Engineering, Peking University, 5 Yiheyuan Road, Beijing 100871, P. R. China

Correspondence to: shangjing@pku.edu.cn

The supporting information has ~~8~~9 pages, 1 table, and 1~~0~~3 figure~~s~~.

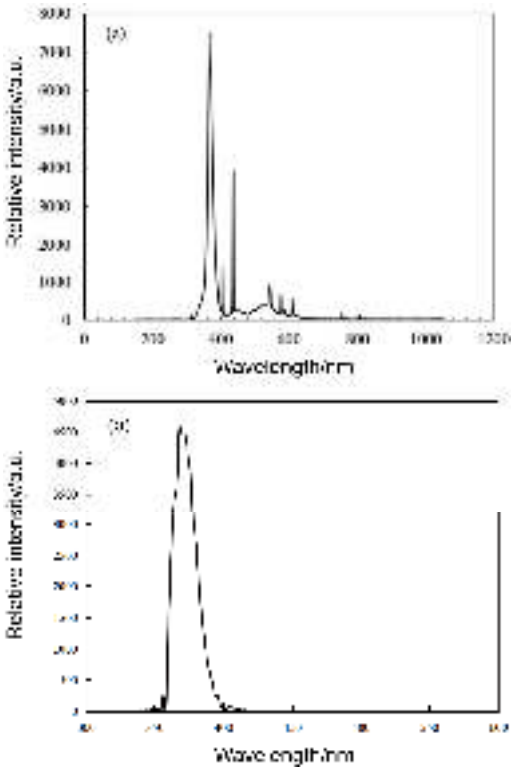

Figure S1. Spectral energy distribution of (a) 365 nm tube lamps and (b) 365 nm LED lamps.

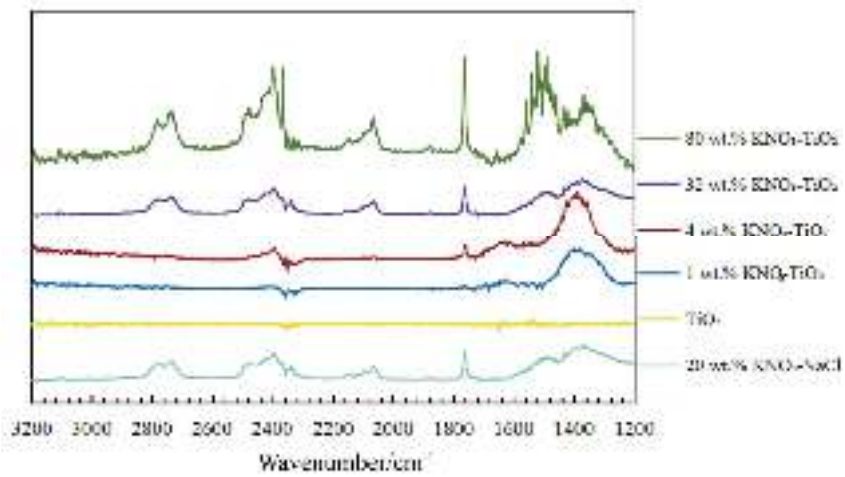

Figure S2. DRIFTS spectra of TiO_2 particles compounded with different mass fractions of KNO_3.

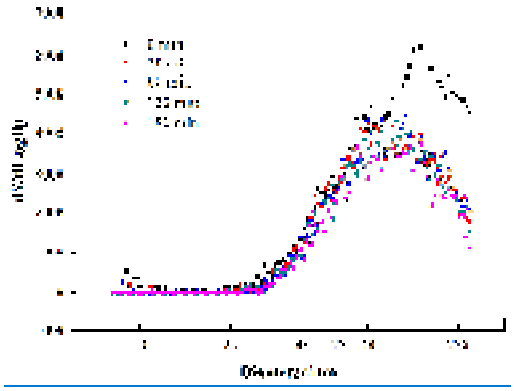

Figure S3. Changes of particle size distribution of 4 wt.% KNO_3-TiO_2 particles in environmental chamber with time.

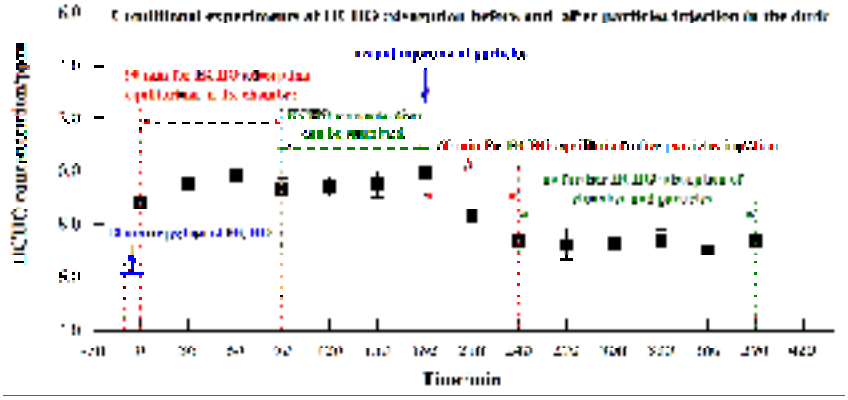

Figure S4. The conditional experiments of HCHO concentration in the environmental chamber in the dark before and after the introduction of particles over time.

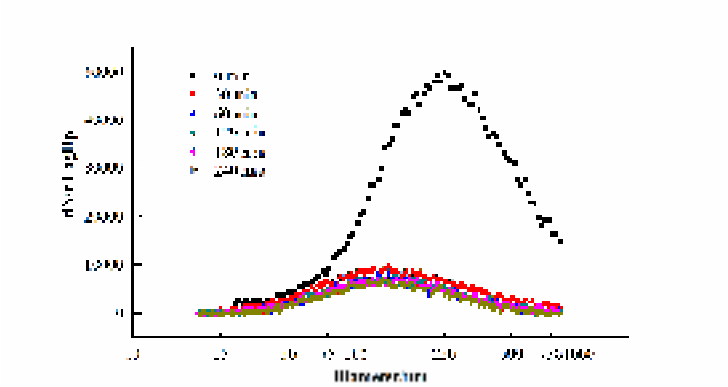

Figure S2. Changes of particle size distribution of TiO_2 particles in environmental chamber with time.

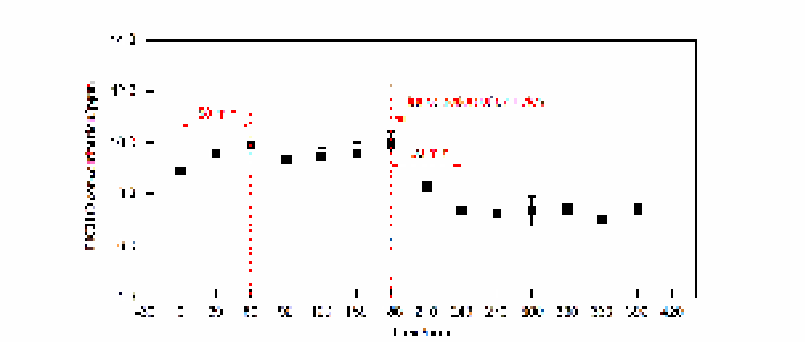

Figure S3. Changes of HCHO concentration in the environmental chamber before and after the introduction of particles over time.

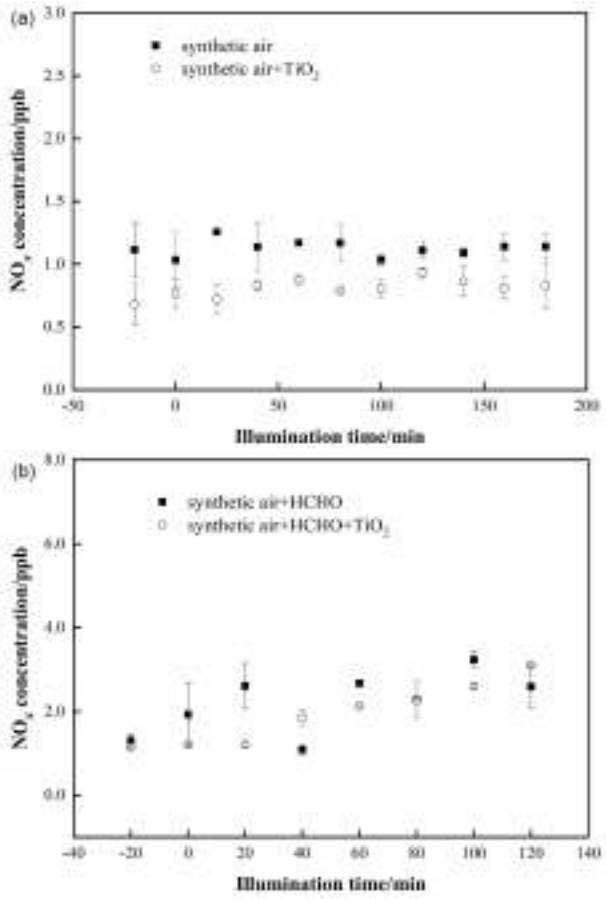

Figure S45. Changes of NO_x concentration in environmental chamber in (a) "synthetic air" and "synthetic air + TiO_2" system, (b) "synthetic air + HCHO" and "synthetic air + HCHO + TiO_2" system. 365 nm tube lamps were used during the blank experiment.

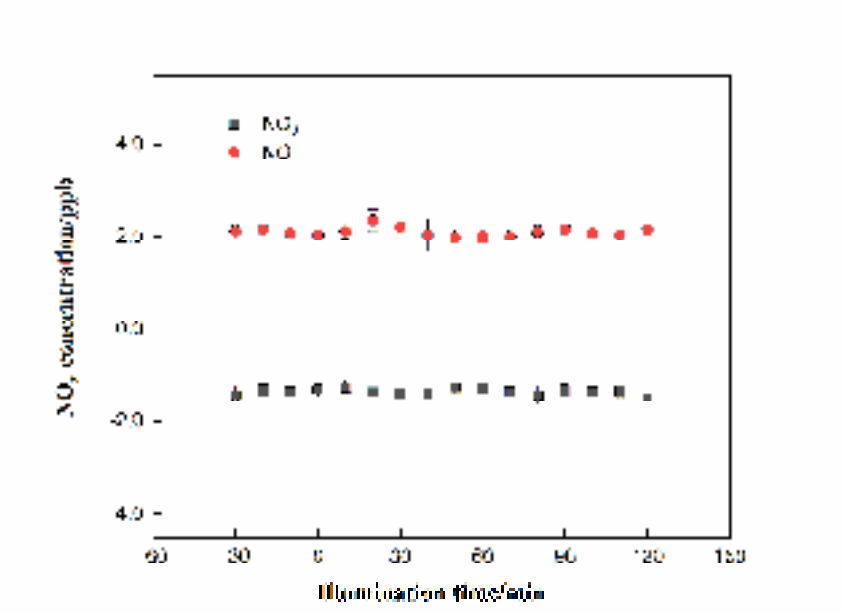

877

878 **Figure S56.** Effect of illumination on the release of NO and NO_2 over 4 wt.% KNO_3-TiO_2 at 293
879 K and 0.8% of relative humidity. 365 nm LED lamps were used during the illumination
880 experiment.

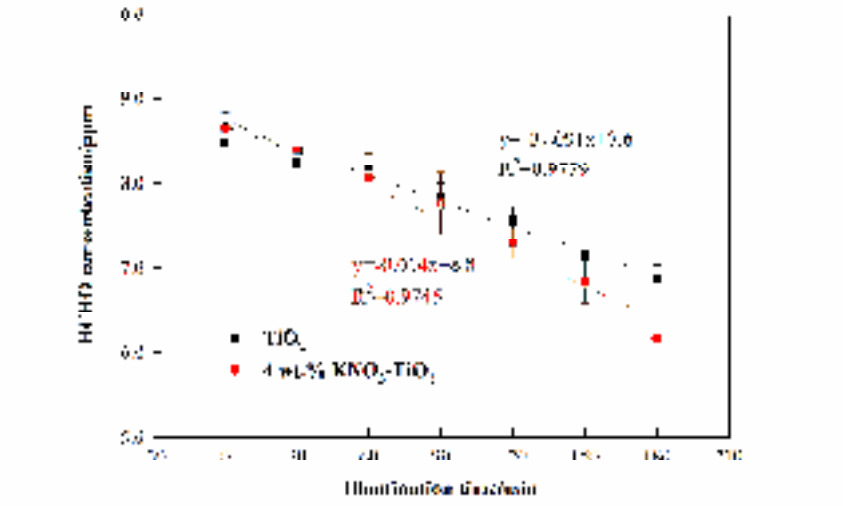

881

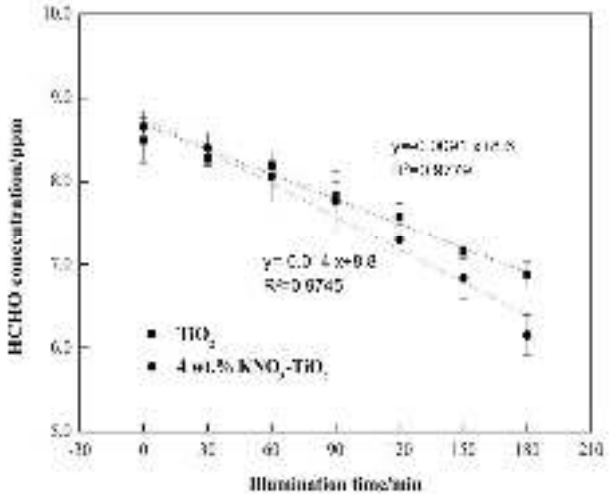

Figure S67. Photodegradation curve of HCHO on TiO_2 and 4 wt.% KNO_3-TiO_2 particles under 365 nm LED lamps at 293 K and 0.8% of relative humidity.

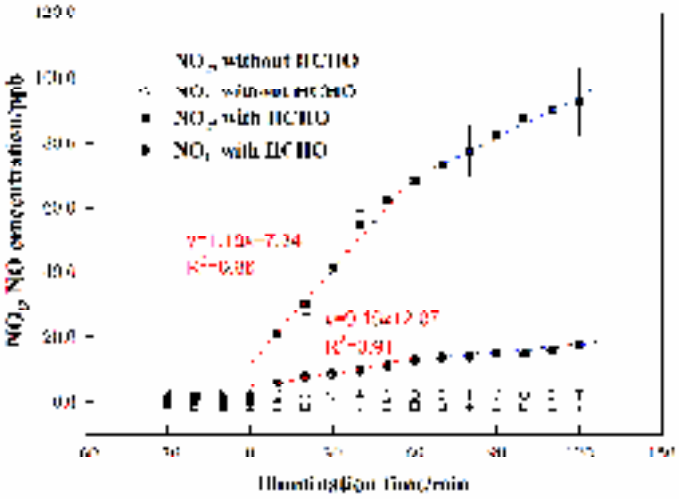

Figure S78. Effect of HCHO on the production of NO and NO_2 over 4 wt.% KNO_3-TiO_2 particles at 293 K and 0.8% of relative humidity. 365 nm LED lamps were used during the illumination experiment. The initial concentration of HCHO was about 9 ppm.

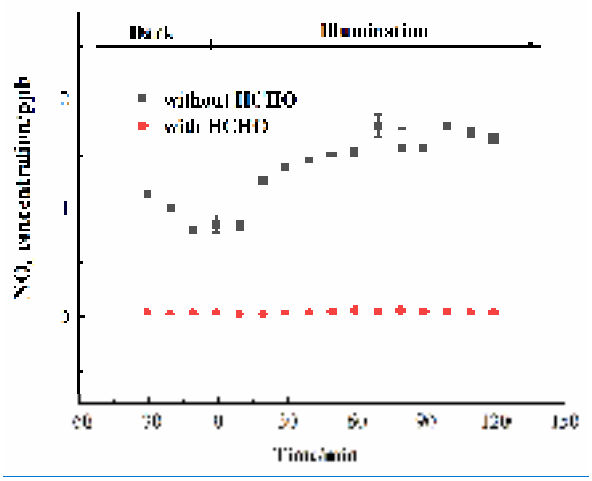

Figure S9. Effect of formaldehyde on the renoxification processes of 4 wt.% KNO_3-SiO_2 particles at 293 K and 0.8% of relative humidity. 365 nm LED lamps were used during the irradiation experiment. The initial concentration of HCHO was about 9 ppm.

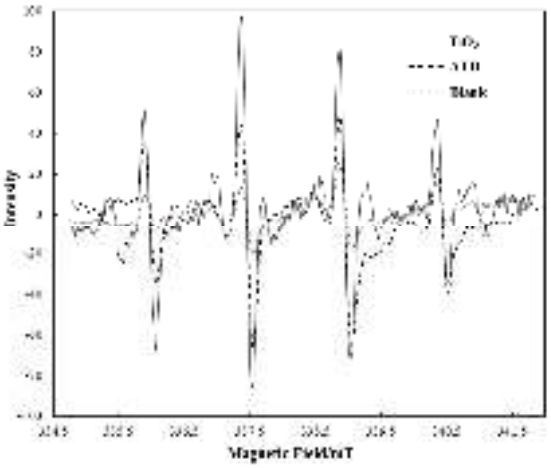

Figure S108. ESR spectra of irradiated TiO_2 and ATD particles.

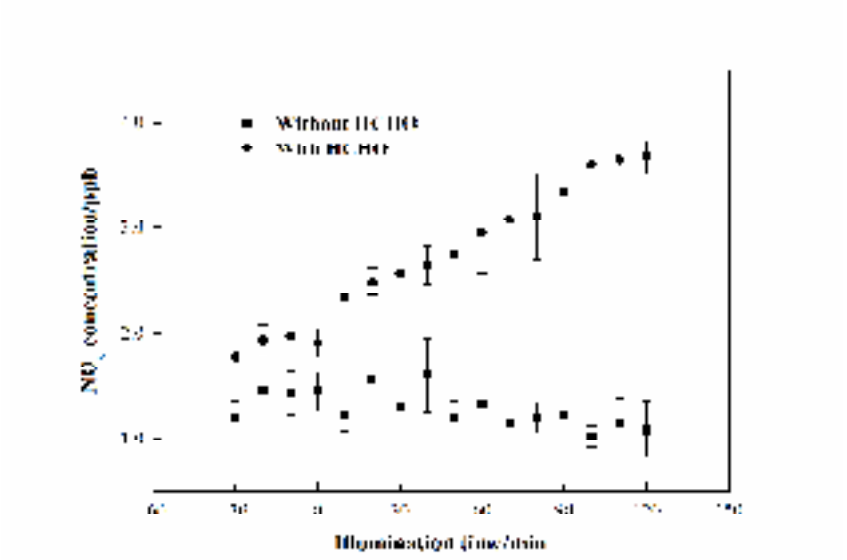

Figure S911. Effect of HCHO on the renoxification processes of Arizona Text Dust (ATD) at 293 K and 0.8% of relative humidity. 365 nm LED lamps were used during the illumination experiment. The initial concentration of HCHO was about 9 ppm.

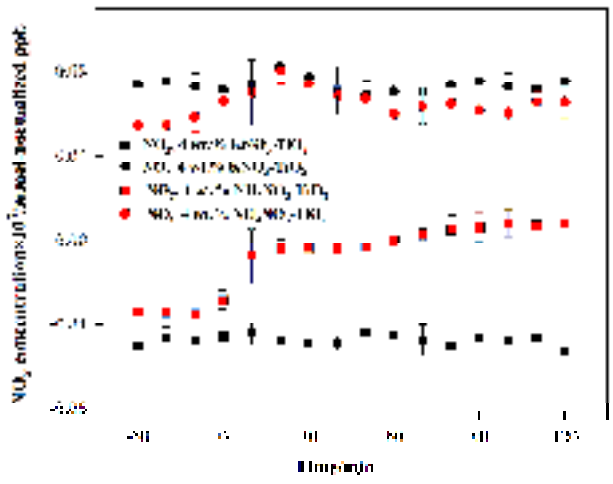

Figure S12. Change of NO_x concentration over 4 wt.% KNO_3-TiO_2 and 4 wt.% NH_4NO_3-TiO_2

particles at 293 K and 0.8% of relative humidity. 365 nm LED lamps were used during the illumination experiment.

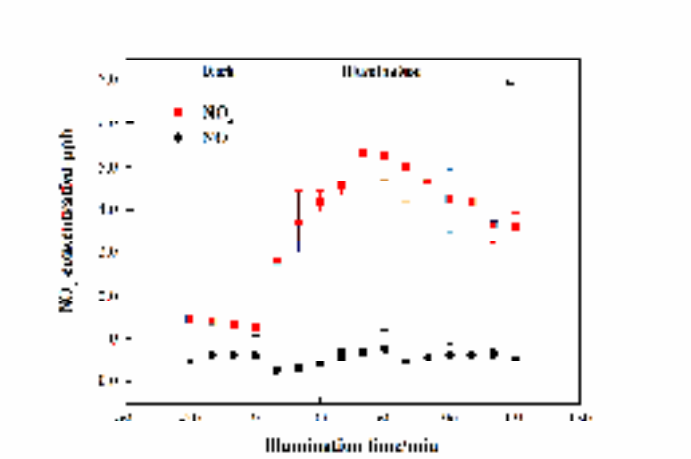

Figure S103. The release of NO_2 and NO with 365 nm LED lamps illumination over 4 wt.% KNO_3-TiO_2 particles at 293 K and 0.8% RH. The initial concentration of HCHO was about 1.0 ppm.

Table S1. Arizona Test Dust (ATD) chemical composition.

Chemical composition	Weight percentage (%)
SiO_2	68-76
Al_2O_3	10-15
Fe_2O_3	2.0-5.0
Na_2O	2.0-4.0
CaO	2.0-5.0
MgO	1.0-2.0
TiO_2	0.5-1.0
K_2O	2.0-5.0

*Loss on Ignition 2-5 %